Development of a Flight Electric Propulsion Diagnostic Package (EPDP) for EP Satellite Platforms

IEPC-2019-345

Presented at the 36th International Electric Propulsion Conference
University of Vienna, Austria
September 15-20, 2019

T. Trottenberg[1], S. I. Böttcher[2], H. Kersten[3], B. Schuster[4],
L. Seimetz[5], A. Spethmann[6], and R. F. Wimmer-Schweingruber[7]
Institute of Experimental and Applied Physics, University of Kiel, 24098 Kiel, Germany

F. Bansemer[8], H. Henkel[9], M. Hesse[10], P. Muller[11], and T. Scott[12]
von Hoerner & Sulger GmbH, Schwetzingen, Germany

and

J. Laube[13]
OHB System AG, Bremen, Germany

This paper reports on the ongoing development of an Electric Propulsion Diagnostic Package (EPDP) for satellites with electric propulsion systems. The diagnostics target the plasma surrounding the spacecraft that is created or dominated by the thruster and its surface modifying effects. The diagnostic package includes a retarding potential analyzer, a plane Langmuir probe, and an erosion sensor. The system is planned to fly for the first time on the Heinrich Hertz satellite, which will be launched in 2022. The spacecraft will be equipped with a pair of HEMP thrusters and a pair of Hall thrusters for redundancy.

Nomenclature

A	= active area of a Langmuir probe
I_e, I_i	= electron and ion currents
e	= elementary charge
k_B	= Boltzmann constant
T_e	= electron temperature
λ_De	= electron Debye length

[1]Research Associate, Plasma Technology, trottenberg@physik.uni-kiel.de
[2]Research Associate, Extraterrestrial Physics, boettcher@physik.uni-kiel.de
[3]Professor, Plasma Technology, kersten@physik.uni-kiel.de
[4]Electrical Engineer, Extraterrestrial Physics, schuster@physik.uni-kiel.de
[5]Mechanical Engineer, Extraterrestrial Physics, seimetz@physik.uni-kiel.de
[6]Research Associate, Plasma Technology, spethmann@physik.uni-kiel.de
[7]Professor, Extraterrestrial Physics, wimmer@physik.uni-kiel.de
[8]Development Engineer, bansemer@vh-s.de
[9]Managing Director, henkel@vh-s.de
[10]Development Engineer, hesse@vh-s.de
[11]Development Engineer, muller@vh-s.de
[12]Development Engineer, scott@vh-s.de
[13]Propulsion Engineer, Propulsion Department, jens.laube@ohb.de

I. Introduction

Spacecrafts often carry sensitive instruments, solar panels and other subsystems that might be disturbed or degraded by the unintended backflow from the applied thruster. This is well known from chemical engines long before the time of electric propulsion (EP) system. In case of conventional engines, exhaust material from the firing thrusters can return to the spacecraft, for example, due to self-scattering.[1] Therefore, it is reasonable and important to ask for such undesired effects in the case of electric propulsion systems, too. The suitability of an electric engine needs to be proven with respect to the effects on the spacecraft.

The Deep Space 1 mission, launched in 1998 and solar electrically propelled by a gridded ion thruster, carried already a diagnostic package with twelve sensors, including quartz crystal microbalances and calorimeters for an assessment of surface deposition or erosion, and a retarding potential analyzer and a planar as well as a spherical Langmuir probe for diagnostics of the plasma environment.[2,3] The in-flight measurements proved the significance of a thruster-induced charge-exchange plasma environment; current densities of $0.1\,\mu\mathrm{A\,cm^{-2}}$ were measured near the thruster exit during the operation of the thruster. One of the findings was that molybdenum sputtered from the thruster grids deposited on the spacecraft surfaces. After 2750 hours of thruster operation, a sensor in direct line-of-sight to the thruster collected about 250 Å, while a shadowed sensor still measured a 25 Å layer.

An in-flight diagnostic system for the assessment of such effects was also part of the SMART-1 mission launched in 2003 that was propelled by a Xenon Hall thruster.[4,5] This electric propulsion diagnostic package consisted of a retarding potential analyzer (RPA), a spherical Langmuir probe (LP), and, serving as contamination sensors, a small solar cell and a quartz microbalance. Essential results of the measurements are summarized in Ref. 3: The measured ion energy distributions of the backflow exhibited a dominant population with energies about 35 eV; but there was also a plateau with approximately 15 % of the peak rate that extended to approximately 60 eV, from where it decreased and vanished at 90 eV. The authors of the above mentioned paper attribute these higher energies to doubly charged ions. The floating cathode (neutralizer) of the Hall thruster attained potentials ranging from −5 V up to +10 V depending on the orientation of the solar panels relative to the spacecraft. This indicates a strong influence of the spacecraft geometry on the potential distribution in its vicinity. The measured erosions have been reported to be small.

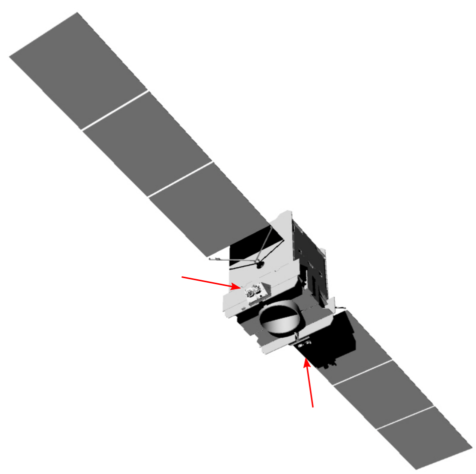

Figure 1. This drawing shows the Heinrich Hertz satellite including solar arrays for power generation, the satellite structure including central tube, outer panels, and the EP thrusters for station keeping. The red arrows indicate the two EP thruster pairs, each pair consisting of a HEMP and a Hall thruster.

In this contribution, we report on a joint collaboration of von Hoerner & Sulger GmbH, OHB System AG, and the Christian-Albrechts-Universität zu Kiel (CAU) for the development of a generic Electric Propulsion Diagnostic Package (EPDP) for satellites propelled by a variety of plasma or ion thrusters, i.e. Hall thrusters, radio-frequency ion thrusters (RIT), or Highly Efficient Multistage Plasma (HEMP) thrusters. The system is planned to fly for the first time on the Heinrich Hertz communications satellite (H2Sat) scheduled to be launched in 2022 (see Fig. 1). The Heinrich Hertz mission, financed by the German Aerospace Center (DLR) and currently being built in Bremen under the lead of OHB as system integrator, aims to explore and test new communication technologies in space at a technical and scientific level. The mission also offers universities, research institutes and industry a platform for conducting numerous scientific and technical experiments. Heinrich Hertz will be equipped with a pair of HEMP thrusters from Thales Electronic Systems GmbH and a pair of Hall thrusters for redundancy (see Fig. 2).

The purpose of the diagnostic package is, similar to the mentioned predecessor systems, an assessment and better understanding of the interaction of the thrusters with the spacecraft, in particular sputter erosion of satellite surfaces and deposition of sputter products on other surfaces of the satellite.

For a characterization of the plasma that causes the erosion and changes the electric field strengths at the surfaces, an arrangement of a retarding potential analyzer and a plane Langmuir probe is used. In the following, this combination will be called the plasma sensor (PS). The retarding potential analyzer allows determining the energy distribution function of the plasma ions. It is equipped with four grids, where the outer grid is always at spacecraft potential and integrated into a slanted surface of the common sensor head. This allows an orientation toward the plume. The Langmuir probe is integrated into another face of the PS (see Fig. 3) and surrounded by a guard ring always kept at the same potential as the probe itself by the probe electronics. This reduces the boundary effects due to the potential discontinuity at the edge of the probe surface by shifting the discontinuity to larger radii; thus, the potential above the (inner) probe surface becomes more homogeneous. The design goal of the probe is to make it part of the body of the spacecraft and avoid complex geometries in terms of the interpretation of the measured data. The erosion sensor (ES) is based on a resistance measurement of a thin conductive layer. The change of the resistance of a silver meander is monitored during the operation of the thrusters, from which the erosion can directly be calculated.

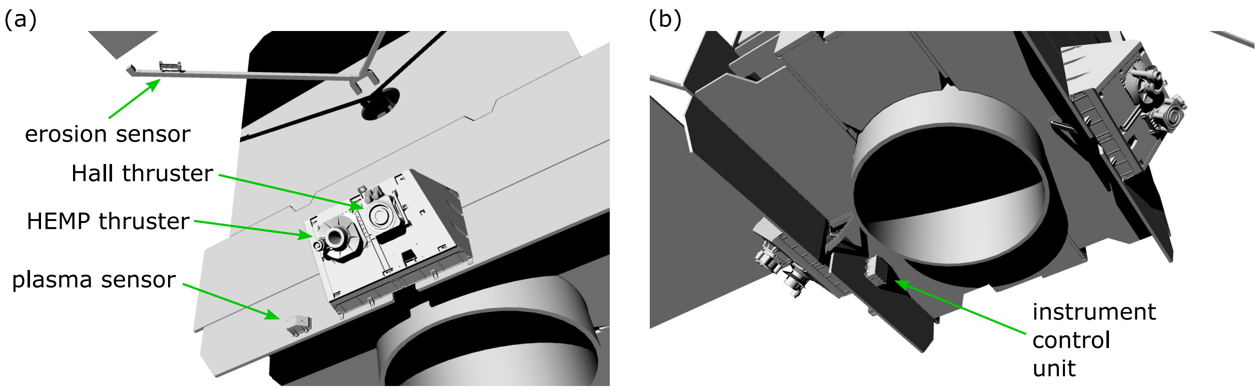

Figure 2. The components of the Electric Propulsion Diagnostic Package (EPDP) on the satellite. (a) The plasma sensor (PS) is mounted on a radiator close to one of the thruster pairs; its retarding potential analyzer is oriented toward the plume. The erosion sensor is attached to one of the solar panel frames. (b) This view shows both thruster pairs. Behind the radiator of the left thrusters, one can see the instrument control unit of the EPDP. The harnesses to to the PS and the ES are not shown.

The two sensors will be located behind the exhaust planes of the thrusters, as can be seen in Fig. 2. The EPDP measures only at two positions on the satellite and can consequently not provide a complete characterization of the plume-surface interaction. To close this gap, modeling of the spacecraft environment is very important.[6] The EPDP is expected to provide reliable data for validation and improvement of numerical models; however, these aspects are not included in this contribution to the conference.

The following section describes the current state of the retarding potential analyzer, the Langmuir probe, and the erosion sensor, which are still under development. Thereafter, in Sec. III, an environment for preliminary tests is presented. Finally, first conclusions are drawn, and the next refinement steps are sketched.

II. Description of the Diagnostics

This section describes in detail the RPA and the LP, which are integrated into the combined plasma sensor, PS, (Fig. 3) and the erosion sensor, ES, with its own housing (Fig. 5).

The EPDP consists of the two sensors PS and ES, an instrument control unit (ICU), and two harnesses that connect the sensors to the ICU, respectively. Figure 2 shows the package (without the harnesses) and

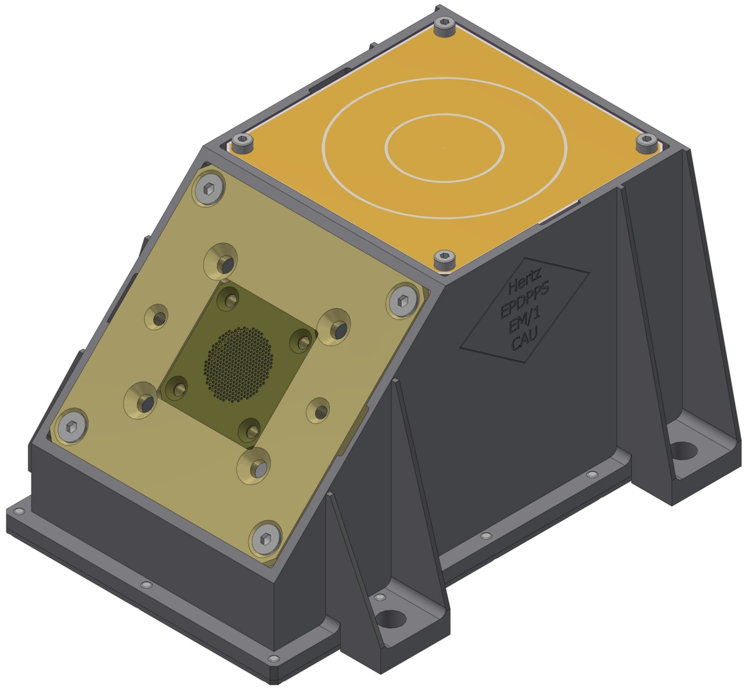

Figure 3. The plasma sensor of the EPDP. One can see the entrance grid of the retarding potential analyzer in the slanted face and the plane Langmuir probe with guard ring on the top face.

how the parts are arranged on the Heinrich Hertz satellite.

The ICU is an electronics box (see Fig. 2(b)) that includes the main electronics of the instrument, particularly all sensor electronics, control, power supply, and the spacecraft interface. It contains a field-programmable gate array (FPGA), the voltage generators, measurement circuits for RPA and LP, and the resistance measurement electronics for the ES. Additionally, there are thermistor electronics measuring temperatures of two thermistors attached to LP and RPA. All voltages are generated from the DC 28 V satellite bus voltage.

The ICU is planned to be mounted behind one of the thruster radiators, i.e. shadowed from the thrusters. The PS is mounted on the same radiator that carries the ICU on its back side at a distance of 55 cm from the thruster exit. The 45° slanted face of the PS, in which the RPA is integrated, points towards the center of the HEMP thruster exit. The erosion sensor is located near one of the solar array panels to provide a realistic measurement of the erosion effects there (see Fig. 2(a)).

A. Retarding Potential Analyzer

An RPA consists essentially of a biased grid placed between the entrance and a collector plate. Only the charged particles with kinetic energies greater than the grid potential are able to overcome the potential barrier and reach the collector. The RPA can therefore be regarded as a high-pass energy filter.

In addition to the mentioned discriminating grid, more grids are necessary in order to obtain meaningful signals at the collector.[7–9] The EPDP RPA comprises four titanium grids, which can be seen in Fig. 4. The first (entrance) grid is electrically and mechanically integrated into the surface of the sensor head and therefore at spacecraft potential. The purpose of this grid is to become electrostatically part of the conductive surface of the satellite without disturbing the ambient plasma. At the same time, most of the plasma electrons are repelled in the plasma sheath between entrance grid and plasma. However, the ions accelerated by the potential drop between plasma and satellite ground will pass through the grid. Electrons with sufficient kinetic energy overcome the potential barrier and can pass through the grid, too. These electrons are to be sorted out electrostatically, otherwise their current onto the collector would partially neutralize the ion current, which we are interested in. In order to repel these electrons, the second (repeller) grid is used; it is negatively biased, e.g. at −20 V. Behind the above mentioned third (discriminator) grid, another electron repelling grid is used. This one reflects ion-induced secondary electrons that are generated at the collector surface by the ions that hit the collector. If these emitted secondary electrons were lost, their current would be misinterpreted as an additional ion current. Obviously, this grid needs to be sufficiently negative with respect to the collector, which is the potential of origin of the secondary electrons. We keep this secondary electron grid at the same negative potential as the plasma electron repeller grid by driving it with the same voltage supply.

As one can see in Fig. 4(b), the three inner grids have greater diameters (19.3 mm) than the entrance grid (14 mm). This accounts for a possible small transversal velocity component of the ions. Trajectories of obliquely entering ions could exceed the radius of the entrance grid. In the chosen design, such ions still pass through the inner grids; at the collector plane, these ions will reach one of the three outer ring segments. A simultaneous measurement of the four collector currents therefore provides information about the direction to the plasma plume.

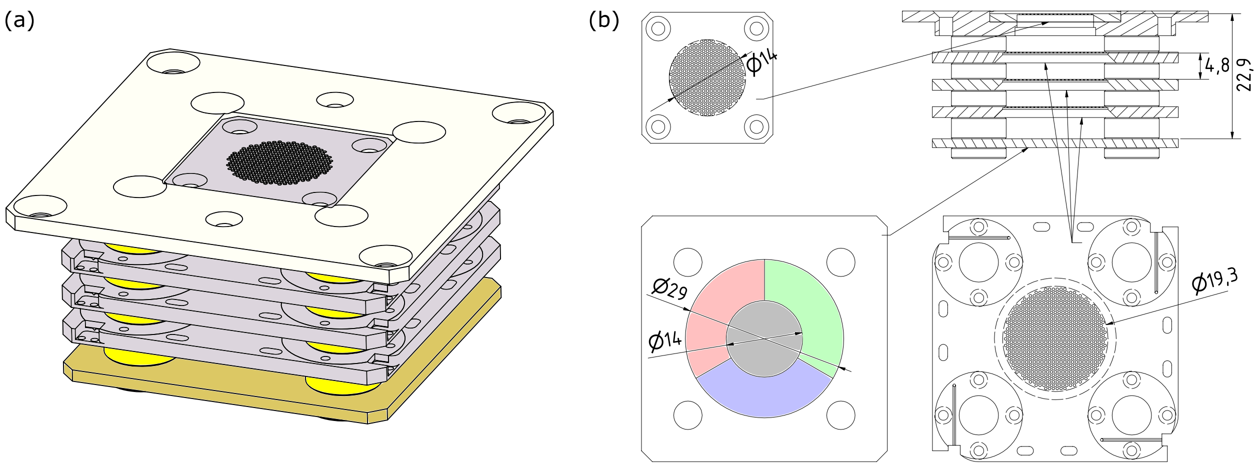

Figure 4. The retarding potential analyzer. (a) The instrument consists of a stack of four titanium grids and a collector plate. (b) The construction drawings show details of the geometry. Note the segmented collector with a central area (gray) and three outer ring segments (colored). The remaining surface of the collector plate (white) is also covered with a conductive layer and grounded. The individual segments are insulated from each other by a narrow trench.

Figure 4 also indicates the dimensions along the instrument axis: the distance from the entrance to the collector is 22.9 mm with a pairwise spacing of 4.8 mm between the inner grids and the collector. The collector plate is divided into four segments. The conductive structures are thin layers of copper (50 μm), nickel (5 μm), and gold (0.1 μm) from bottom up. The center segment collects the ions that traverse the grid system perpendicularly to the grids. In case of highly directed ions, only a small part of the current would reach the outer segments. But if there is a deviation of the incident angles from this ideal case, the three outer segments would collect different currents in an asymmetric manner.

B. Plane Langmuir Probe

The design and the choice for a probe type, i.e. planar, cylindrical, or spherical, is a consequence of the expected plasma densities. We expect densities of $n_\mathrm{e} = (5 \times 10^{10} \dots 1 \times 10^{13})\,\mathrm{m}^{-3}$. This wide density range, which extends over more than two orders of magnitude, has two major consequences for the probe design:

First, the screening lengths of the plasma have to be considered; the screening length of a plasma is known as the Debye length. In our case of supersonically streaming ions in the sheath that surrounds big objects in contact with plasma or immersed in plasma, the Debye length

$$\lambda_\mathrm{De} = \left(\frac{k_\mathrm{B} T_\mathrm{e}}{n_\mathrm{e} e^2} \right)^{\frac{1}{2}} \tag{1}$$

of the electrons is the relevant quantity and results from the electron density n_e and the electron temperature T_e. The constants e and k_B are the elementary charge and the Boltzmann constant. For the expected plasma densities, the shielding length becomes $\lambda_\mathrm{De} = 4\,\mathrm{mm} \dots 6\,\mathrm{cm}$, assuming an electron temperature of $k_\mathrm{B} T_\mathrm{e} = 3\,\mathrm{eV}$.

Cylindrical or spherical designs require a mounting at a distance from other objects of the spacecraft greater than the shielding length. Otherwise, the probe would measure in a space charge region with complicated geometry that makes the evaluation of the collected data very difficult. A mounting of a spherical or cylindrical probe on a sufficiently long rod would make the diagnostic mechanically much more challenging and heavier.

In case of a plane probe that is quasi-integrated into the spacecraft surface (actually into the EPDP sensor head), the required probe theory is much simpler. With the same objective, the actual probe surface is surrounded by a ring shaped surface in the same plane that is kept at the same potential as the active probe surface (guard ring) by the probe electronics. This reduces the boundary effects by shifting the effective edge to larger radii. The probe therefore comes closer to the ideal case of (a cutout of) an infinite plane without boundary.

Second, the expected currents have to be considered. A cylindrical probe consisting of a wire would have a much too small surface area A, and the currents would become extremely small. On the other hand, the foreseen planar probe has an effective surface of $A = 3.1\,\mathrm{cm}^2$, the currents for the expected plasma densities (see above) are in the range $I_\mathrm{e} = 0.4\,\mu\mathrm{A} \ldots 90\,\mu\mathrm{A}$ and $I_\mathrm{i} = 2\,\mathrm{nA} \ldots 0.5\,\mu\mathrm{A}$, which sets the requirements for the electronics.

These are two strong reasons in favor of the planar design of the Langmuir probe.

This kind of planar probe with guard ring is often called Faraday probe in the context of electric propulsion.[10] However, in those cases it is used as an instrument for the determination of ion beam current densities, so to speak as a simplified Faraday cup, but here, we use it as a plasma diagnostic tool, and the notion of a plane Langmuir probe therefore describes its function much better.[11] A plane Langmuir probe was also used in the Deep Space 1 mission.[3]

The plane Langmuir probe is integrated in the PS, which also houses the retarding potential analyzer (Fig. 3). The probe is basically a printed circuit board: it consists of a rigid polyimide laminate carrier with conductive segments for the circular active probe surface (diameter 20 mm) and an additional surrounding potential ring, or guard ring, with an outer diameter of 42 mm and a small but deep gap between the two segments, as can be seen in Fig. 3. The conductive structures are manufactured in the same way as the RPA collector surfaces. The plate is directly mounted into the sensor head chassis.

C. Erosion Sensor

The purpose of the erosion sensor is to measure the erosion rate of surface material in the presence of a plasma environment. The key physical effect to be measured is the sputtering of metallic silver from an exposed detector surface due to bombardment by the particles emitted by the HEMP thruster.

The erosion sensor is not part of the previously described plasma sensor head. It is separately mounted on the spacecraft frame that carries the solar panels and is connected via a harness to the electronics box, see Fig. 2. This position of the erosion sensor is chosen to monitor the erosion rate at a critical surface near the solar panels, e.g. the solar panel interconnects.

Simulations were performed by OHB using ray-tracing techniques to extrapolate the plasma properties at a specific distance from the thruster-exit to the far-field, where the spacecraft surfaces are located. Under ordinary thruster operation and for a silver surface at the specified position, these simulations predict a yearly erosion rate within the measurement range of the sensor. One purpose of the EPDP erosion sensor is to confirm or reject the calculated erosion rate and modeling approach. Also it provides a more in-depth view of the erosion mechanisms after each consecutive thruster cycle.

The measurement principle of the erosion sensor is based on a resistance measurement of a thin silver layer. By measuring its resistance change over time, the erosion rate can be calculated. The silver layer in its current design is a $2\,\mu$m thick, 1 mm wide, and 180 cm long meander, extending over an area of 2 cm $\times$ 10 cm on a rectangular ceramic substrate plate, which results in a resistance of approximately $15\,\Omega$. The meander structure becomes necessary to increase the sensor resistance to a reasonable value compared to the wire resistance of the harness.

The erosion sensor is depicted in Fig. 5. The rectangular surface in the drawing is the ceramic plate with the conductive thin film path. To lower thermal stress and prevent cracks of the ceramic, it is fixated by metallic springs. The erosion sensor is connected through a D-Sub connector and is mounted to the spacecraft by M4 screws.

For the resistance measurement, four wires are used to remove the influence of the connecting wires by separating the stimulus wires from the sensing wires. Since the expected temperatures can range from

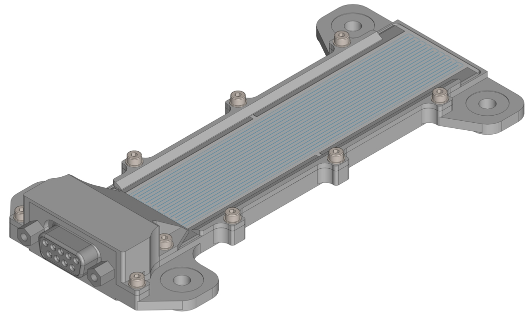

Figure 5. The erosion sensor consists of a ceramic plate with a thin silver meander and a housing, in which the plate is held in place with metallic springs. A D-Sub connector provides the electrical interface.

approximately $-80\,^{\circ}\mathrm{C}$ to $+110\,^{\circ}\mathrm{C}$, thermal effects are subtracted from the signal by using information from a thermistor attached to the ceramic. Possible radio-frequency disturbance from the thruster and other electromagnetic interference sources are filtered out from the measurement signal by the measurement electronics. Also a possible strong DC current flow produced by the HEMP thruster and solar effects have to be considered, which may generate a DC offset in the measurement signal. The key solution is to employ an AC measurement principle.

Several implementations are currently under development, and first investigations of the erosion sensor performance in a plasma environment are planned for 2019 and are intended to be presented in a follow-up publication.

III. Test Environment

In contrast to typical measurements in test chambers, the three sensors onboard the satellite will not be exposed directly to the beam as was explained in Sec. II (see Fig. 1). The sensors measure the dilute backflow from the thruster plume that alters or dominates the plasma surrounding the spacecraft. In order to create a plasma environment similar to the situation aboard the satellite, we use an ion beam from a broad-beam ion source that has been described in detail in various publications[12,13] and place the plasma sensor at a position outside the beam so that the beam will not strike the diagnostics.

The beam creates a population of slow ions via charge-exchange collisions with neutral gas. This population expands radially by drift and diffusion and fills the entire cylindrical chamber. The measurements reported in this paper are performed in argon at a pressure of some 10^{-2} Pa. The hot and the cold ions together with electrons that are created at the beam dump by ion-induced secondary electron emission, or escape from the ion source, or are optionally introduced by a hot filament, form a quasi-neutral plasma.[13]

Figure 6 shows a sketch of the 160 cm long test chamber where the ongoing in-house testing is being performed. The grid system of the broad-beam ion source for ion extraction and acceleration consists of three spherically curved graphite grids with a curvature radius of 300 mm and a diameter of 125 mm. An antenna emits approximately 360 W of 2.4 GHz microwaves into the source chamber. The potential in the ceramic source chamber is raised by an inner ring anode and defines the accelerating potential and strong electric field in the grid system. The anode potential is ≤ 1200 V. The ion beam leaves the source at one end of the vacuum chamber, passes through a screen, traverses the chamber and ends after a length of approximately 140 cm at the opposed beam dump. The screen reduces the beam diameter from 125 mm to 80 mm.

The EPDP plasma sensor head is mounted on the turnable and laterally movable platform together with a cylindrical Langmuir probe and a Faraday cup, which do not belong to the EPDP. The cylindrical Langmuir probe is used for a characterization of the plasma in front of the EPDP sensor head, and, when moved by

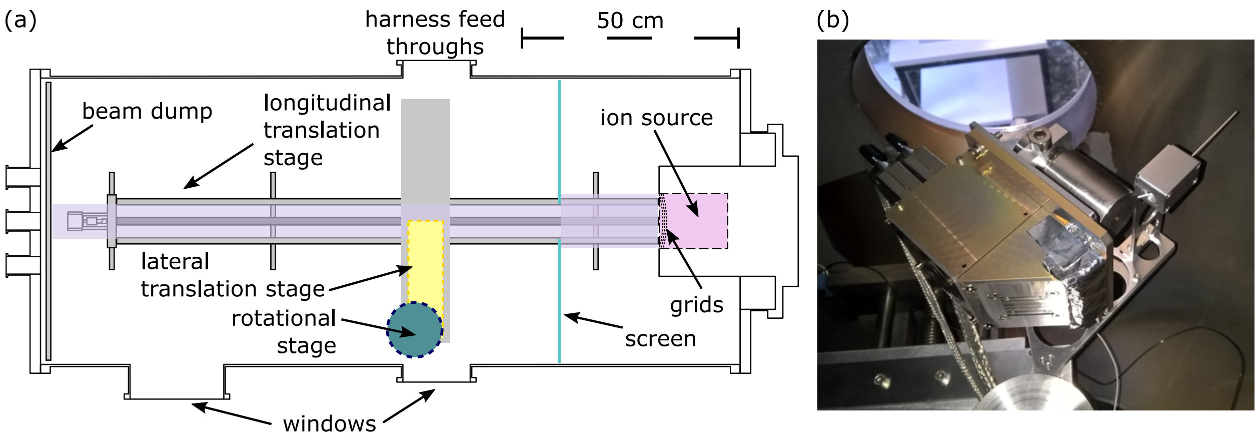

Figure 6. In-house testing of the EPDP in the chamber at the University of Kiel. (a) The sketch shows the geometrical arrangement of ion beam and the EPDP plasma sensor head. The EPDP is mounted together with additional diagnostics on the rotational stage. (b) The photograph of the rotational stage shows the sensor head in the front and behind it a Faraday cup and cylindrical Langmuir probe for beam and plasma characterization.

the lateral translation stage into the ion beam, the plasma potential of the beam. The Faraday cup can also be moved into the beam in order to measure the absolute ion flux density in the beam.

The RPA can be moved into the beam and rotated about its vertical axis until it faces the beam source; small rotations allow the quasi-parallel ion beam to enter the grids at variable angles. This configuration will be used for a characterization of the angular sensitivity of the sensor.

However, to mimic the situation on the satellite, the RPA is moved to a position 18 cm away from the beam axis and rotated until its axis points perpendicularly to the beam. Figure 7(a) shows the measured raw data from a test measurement at a beam energy of 1.2 keV. While the black curve represents the current at the central (main) collector area, the colored curves are for the three eccentric ring segments. As expected, the latter currents are significantly smaller, which indicates that the ions are entering the RPA with a narrow angular distribution centered about the instrument axis.

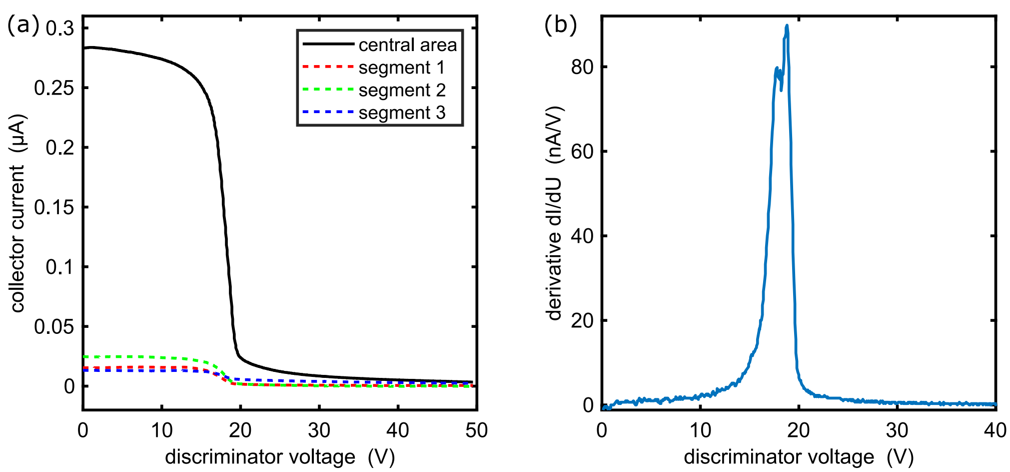

Figure 7. Example of a measurement with the EPDP retarding potential analyzer (RPA). The RPA is directed perpendicularly to the beam at a distance of 18 cm. The beam ions have a kinetic energy of 1200 eV. The two electron repeller grids were at a potential of −20 V. (a) Currents collected by the four collector areas. (b) The first derivative of the current at the central collector area can be interpreted as the ion energy distribution function. Its peak value is then at 18.8 eV.

One can clearly distinguish to regimes: First, the regime of higher currents for screen grid voltages below approximately 15 V, and, second, the regime of almost vanishing currents for voltages above approximately 20 V. This indicates that the ion energies are between 15 eV and 20 eV.

The first derivative, shown in Fig. 7(b), can be interpreted as the ion energy distribution function: The

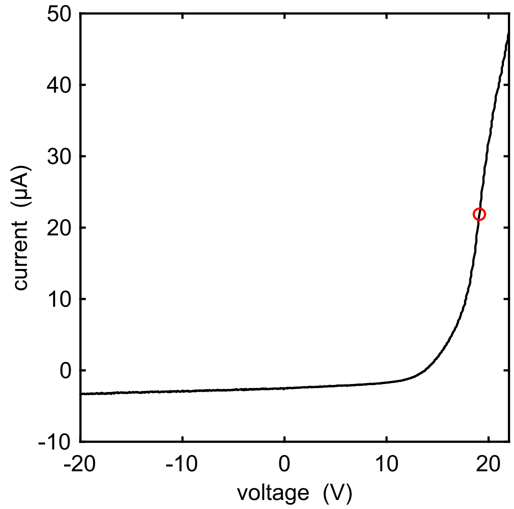

Figure 8. Example of a measurement with the plane EPDP Langmuir probe (LP). The inflection point, indicated by the red circle, indicates the plasma potential at $+19.1$ V relative to the chamber ground potential.

retarding potential in volts corresponds to the energy of the singly charged ions in eV. The most abundant energy is found at 18.8 eV.

Figure 8 shows data taken with the Langmuir probe at the same beam conditions and without changing position and orientation of the sensor head. Due to the geometry of the sensor head, the surface normal of the Langmuir probe was at an angle of 45 degrees to the line from the sensor head to the beam.

The setup is therefore similar to the one in space with the HEMP and Hall thrusters. However, in our experimental setup we did not use a neutralizer (or the optional hot filament).

The characteristic shows a clear inflection point that indicates the plasma potential at $+19.1$ V (Fig. 8). This corresponds to the ion energies measured by the RPA and can be explained in the following way: The ions detected by the RPA originate in the beam, which is at the plasma potential. The ions likely reach the RPA without collisions and therefore have an energy of approximately 19 eV.

IV. Concluding Remarks and Next Steps

This paper reported on the development of a diagnostic package for the Heinrich Hertz satellite, which will be launched in 2022. The three diagnostics, a retarding potential analyzer, a plane Langmuir probe, and an erosion sensor, were described as far as it was reasonable in this early stage of the development. The active electronic components, which will be installed in the instrument control unit apart from the two sensor units, were not considered in this report; we still did not perform any tests of the electronics in a plasma environment.

However, the RPA and the LP were operated in a chamber where an ion-beam generated secondary plasma served as an imitation of the backflow from a thruster to the spacecraft. For this test, laboratory electronics were used instead of the later EPDP electronics. The results show the expected interrelation between plasma potential and ion energy, which indicates that the detected ions stem from charge-exchange collisions of the beam (plume) ions with neutral gas atoms. These ions 'fall' from the secondary plasma down to the grounded walls and the diagnostics; the situation corresponds to charge-exchange ions created behind the thruster which flow through the thruster-induced environment plasma back to the spacecraft. This is in agreement with the in-flight measurements from the Deep Space 1 mission[2] as well as the SMART-1 mission.[4]

The next step will be a test at the Thales Electronic Systems test facility in Ulm with a HEMP thruster of the type that will fly on the Heinrich Hertz satellite. There, distance and orientation of the EPDP plasma sensor head to the thruster will be chosen representative for those on the spacecraft. Even though the ion backflow might be strongly affected by chamber effects, such a test can give confidence in the estimations of the thruster-induced plasma from simulations. Moreover, HEMP thrusters exhibit self-excited oscillations of the discharge current (several 10 kHz) that could be challenging for the diagnostics or need to be considered in the development of the EPDP electronics.

Further tests in the CAU laboratory include tests of the erosion sensor in a plasma environment. Both erosion and contamination (deposition) can be induced in the ion beam chamber. Furthermore, systematic manipulations of the beam potential by means of a hot filament and the plasma density by reducing the microwave power of the ion source are planned. Thus, the behavior of RPA and LP at different ion energies and plasma densities can be investigated.

Acknowledgments

This work is financially supported by European Space Agency (ESA) under GSTP Contract No. 4000126205/19/NL/RA. Parts of this work have been funded by the Horizon 2020 Framework Programme of the European Union.

References

[1] P. T. Chen, S. Thomson, and M. S. Woronowicz, "Applying Contamination Modeling to Spacecraft Conventional Propulsion System Designs and Operations," *J. Spacecr. Rockets*, vol. 38, pp. 388–392, 2001.

[2] J. Wang, D. E. Brinza, D. T. Young, J. E. Nordholt, J. E. Polk, M. D. Henry, R. Goldstein, J. J. Hanley, D. J. Lawrence, and M. Shappirio, "Deep Space One Investigations of Ion Propulsion Plasma Environment," *J. Spacecr. Rockets*, vol. 37, pp. 545–555, 2000.

[3] D. Brinza, J. Wang, J. Polk, and M. Henry, "Deep Space 1 Measurements of Ion Propulsion Contamination," *J. Spacecr. Rockets*, vol. 38, pp. 426–432, 2001.

[4] J. Gonzlez del Amo, D. Estublier, C. Koppel, M. Capacci, M. Tajmar, and A. Passaro, "Spacecraft/thrusters interaction analysis for Smart-1," in *29th International Electric Propulsion Conference, Princeton, New Jersey, U.S.A.*, p. IEPC–2005–003, 2005.

[5] M. Capacci, G. Matticari, G. Noci, A. Severi, and D. Borie, "An Electric Propulsion Diagnostic Package for the Characterization of the Plasma Thruster/Spacecraft Interactions on STENTOR Satellite," in *35th AIAA/ASME/SAE/ASEE Joint Propulsion Conference, Los Angeles, California, USA*, p. AIAA–1999–2277, 1999.

[6] M. Tajmar, J. Gonz-Uuml, and A. Hilgers, "Modeling of Spacecraft-Environment Interactions on SMART-1," *J. Spacecr. Rockets*, vol. 38, pp. 393–399, 2001.

[7] T. Baloniak, R. Reuter, C. Fltgen, and A. von Keudell, "Calibration of a miniaturized retarding field analyzer for low-temperature plasmas: geometrical transparency and collisional effects," *J. Phys. D: Appl. Phys.*, vol. 43, p. 055203, 2010.

[8] S. D. Johnson, M. M. El-Gomati, and L. Enloe, "High-resolution retarding field analyzer," *J. Vac. Sci. Technol. B*, vol. 21, pp. 350–353, 2003.

[9] J. A. Simpson, "Design of Retarding Field Energy Analyzers," *Rev. Sci. Instrum.*, vol. 32, pp. 1283–1293, 1961.

[10] D. L. Brown, M. L. R. Walker, J. Szabo, W. Huang, and J. E. Foster, "Recommended Practice for Use of Faraday Probes in Electric Propulsion Testing," *J. Propul. Power*, vol. 33, pp. 582–613, 2017.

[11] H. M. Mott-Smith and I. Langmuir, "The theory of collectors in gaseous discharges," *Phys. Rev.*, vol. 28, pp. 727–763, Oct 1926.

[12] M. Zeuner, F. Scholze, H. Neumann, T. Chass, G. Otto, D. Roth, A. Hellmich, and B. Ocker, "A unique ECR broad beam source for thin film processing," *Surf. Coat. Technol.*, vol. 142–144, pp. 11–20, 2001.

[13] T. Trottenberg, A. Spethmann, J. Rutscher, and H. Kersten, "Non-electrostatic diagnostics for ion beams and sputter effects," *Plasma Phys. Control. Fusion*, vol. 54, p. 124005, 2012.